Original Article

Increased Myocardial Oxygen Consumption Reduces Cardiac Efficiency in Diabetic Mice

Ole-Jakob How,[1] Ellen Aasum,[1] David L. Severson,[2] W.Y. Anna Chan,[3] M. Faadiel Essop,[3] and Terje S. Larsen[1]

Altered cardiac metabolism and function (diabetic cardiomyopathy) has been observed in diabetes. We hypothesize that cardiac efficiency, the ratio of cardiac work (pressure-volume area [PVA]) and myocardial oxygen consumption (MVo_2), is reduced in diabetic hearts. Experiments used ex vivo working hearts from control *db/+*, *db/db* (type 2 diabetes), and *db/+* mice given streptozotocin (STZ; type 1 diabetes). PVA and ventricular function were assessed with a 1.4-F pressure-volume catheter at low (0.3 mmol/l) and high (1.4 mmol/l) fatty acid concentrations with simultaneous measurements of MVo_2. Substrate oxidation and mitochondrial respiration were measured in separate experiments. Diabetic hearts showed decreased cardiac efficiency, revealed as an 86 and 57% increase in unloaded MVo_2 in *db/db* and STZ-administered hearts, respectively. The slope of the PVA-MVo_2 regression line was increased for *db/db* hearts after elevation of fatty acids, suggesting that contractile inefficiency could also contribute to the overall reduction in cardiac efficiency. The end-diastolic and end-systolic pressure-volume relationships in *db/db* hearts were shifted to the left with elevated end-diastolic pressure, suggesting left ventricular remodeling and/or myocardial stiffness. Thus, by means of pressure-volume technology, we have for the first time documented decreased cardiac efficiency in diabetic hearts caused by oxygen waste for noncontractile purposes. *Diabetes* 55: 466–473, 2006

Cardiac efficiency is the ratio between energy output (work) and energy input (myocardial oxygen consumption [MVo_2]) for the heart. Currently, the most accepted definition of total cardiac work is pressure-volume area (PVA), the sum of external mechanical work and the potential energy triangle (1). Importantly, MVo_2 is linearly related to PVA. Extrapolation of this linear relationship to 0 work gives unloaded (PVA independent) MVo_2, the oxygen cost of excitation-contraction coupling and basal metabolism. Furthermore, the inverse slope of the MVo_2-PVA relationship defines the contractile efficiency.

Recently, How et al. (2) demonstrated that pressure-volume loops and resulting determinations of PVA can be obtained with ex vivo perfused working mouse hearts, using a combined micromanometer (pressure)-conductance (volume) catheter. A fiber-optic oxygen probe gave simultaneous measurements of MVo_2. An elevation in perfusate fatty acid concentration resulted in augmented fatty acid oxidation and reduced cardiac efficiency (increased MVo_2 with no change in work), manifested as increased unloaded MVo_2 (2).

Perfused hearts from *db/db* mice, a monogenic model of type 2 diabetes with obesity and insulin resistance, have been characterized as having an early increase in fatty acid oxidation that precedes the onset of contractile dysfunction (3). Because elevated rates of fatty acid oxidation produce a decrease in cardiac efficiency in control hearts (2), the objective of the current investigation was to test the hypothesis that cardiac efficiency will be reduced in diabetic *db/db* hearts because of enhanced rates of fatty acid oxidation (3). Accordingly, *db/db* hearts were perfused with both low and high concentrations of fatty acids (palmitate) in the perfusate. Moreover, comparative studies were performed with perfused hearts from a model of insulin-deficient type 1 diabetes, produced by the administration of streptozotocin (STZ) to control (*db/+*) mice (4). Both type 1 and type 2 diabetic hearts exhibited reduced cardiac efficiency, a characteristic that may have significant pathophysiological implications.

RESEARCH DESIGN AND METHODS

Male C57BL/KsJ-lepr^{db}/lepr^{db} type 2 diabetic (*db/db*) mice and their nondiabetic heterozygote littermates (*db/+*) were purchased from M&B (Ry, Denmark) and used for investigations of cardiac efficiency and ventricular function at 12–13 weeks of age. The same mouse strains from Harlan (Oxon, U.K.) were used for measurements of myocardial metabolism at the University of Tromsø and mitochondrial respiration at the University of Cape Town. All animals were treated according to the guidelines on accommodation and care of animals formulated by the European Convention for the Protection of Vertebrate Animals Used for Experimental and Other Scientific Purposes. Mice were housed at 23 ± 1°C on a 12-h light/dark cycle and given ad libitum access to food and water. Type 1 (insulin-deficient) diabetes was induced in 10-week-old *db/+* mice by injection of a total cumulative dose of 210 mg/kg i.p., which was administered as three individual doses delivered over 3 consecutive days (4,5). The animals were killed and hearts perfused after 2 weeks, and only the animals that showed significantly elevated plasma glucose concentration were included.

Cannulation and instrumentation of the heart. After intraperitoneal injection of heparin (100 units), animals were anesthetized with sodium pentobarbital, after which the heart was quickly excised and cannulated for perfusion in the working mode, using Krebs-Henseleit buffer (KHB) buffer with 11 mmol/l glucose as well as albumin-bound fatty acids as energy substrates (2). A 1.4-F micromanometer-conductance catheter (Millar Instru-

From the [1]Department of Medical Physiology, Institute of Medical Biology, Faculty of Medicine, University of Tromsø, Tromsø, Norway; the [2]Department of Pharmacology and Therapeutics, Faculty of Medicine, University of Calgary, Calgary, Alberta, Canada; and the [3]Hatter Institute for Cardiology Research, Faculty of Medicine, Cape Town, South Africa.

Address correspondence and reprint requests to Ole-Jakob How, Department of Medical Physiology, Institute of Medical Biology, Faculty of Medicine, University of Tromsø, N-9037 Norway. E-mail: ole-jakob.how@fagmed.uit.no.

Received for publication 6 September 2005 and accepted in revised form 7 November 2005.

KHB, Krebs-Henseleit buffer; MVo_2, myocardial oxygen consumption; PVA, pressure-volume area; STZ, streptozotocin.

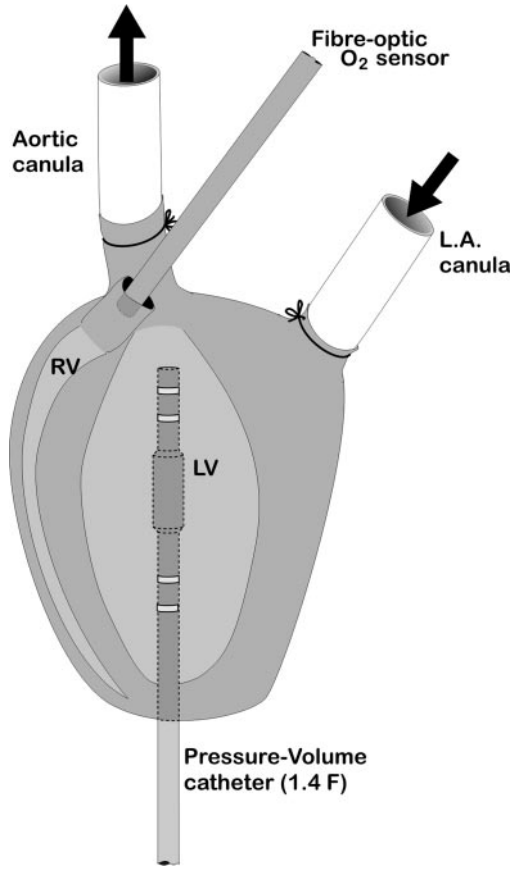

FIG. 1. Schematic of the isolated working mouse heart, showing the position of the pressure-volume catheter and oxygen probe in the left ventricle and pulmonary trunk, respectively. L.A., left atrial; LV, left ventricle; RV, right ventricle.

ments, Houston, TX) was inserted into the left ventricle via the apex of the heart, while a fiber-optic oxygen probe (FOXY-AL300; Ocean Optics, Duiven, the Netherlands) was placed in the pulmonary trunk for on-line recording of the partial oxygen pressure in the coronary effluent (Fig. 1) (2).

Experimental protocol. During stabilization, the initial filling pressure (preload) was set to 8 mmHg; the afterload column was set to a height corresponding to 50 mmHg (2). The hearts were initially perfused with KHB buffer containing 0.3 ± 0.1 mmol/l fatty acids. Steady-state PVA-MVo_2 relationships, and other indexes of ventricular function, were obtained over a wide range of workloads by stepwise changes in the hydrostatic pressure of the preload (3–12 mmHg) and afterload (35–65 mmHg) columns. The concentration of palmitate was subsequently increased to 1.4 ± 0.1 mmol/l over a 5-min period. Thereafter, new measurements of PVA-MVo_2 relationships were performed as described above.

Measurements of left ventricular mechanical function. Left ventricular performance at different workloads was calculated from the pressure-volume loops, which were recorded by a Power Lab Chart 5 data acquisition system (AD Instruments) and analyzed by software accompanying the Millar pressure-volume catheter (PVAN 2.9). In addition, ventricular function and contractility (obtained by a preload occlusion) were determined at baseline steady-state loading conditions before and immediately after the buffer replacement.

Left ventricular volume was assessed by the conductance catheter and calculated as described previously (2). Parallel conductance was assessed by the saline dilution technique described by Baan et al. (6); a bolus (30 μl) injection of hypertonic solution (KHB with added 1% NaCl) was injected in the preload line for achieving an offset in the volume signal. The injections produced only a transient reduction in cardiac function and did not affect buffer electrolyte composition as a result of the high volume (~50 ml) of the perfusate.

Cardiac efficiency. Cardiac efficiency is the ratio between cardiac work (PVA) and MVo_2. PVA is derived from the sum of external stroke (mechanical) work and the potential energy triangle (1). Stroke work was calculated by integrating the pressure-volume loop, whereas the potential energy triangle was assessed by a temporary occlusion of the preload line at each steady state. This occlusion was performed to determine end-systolic and end-diastolic pressure-volume relationships. The volume intercept of these relationships is defined as V_0. PVA was calculated according formula: PVA = SW + $[P_{ES} \times (V_{ES} - V_0)/2] - [P_{ED} \times (V_{ED} - V_0)/4]$ in accordance with Korvald et al. (7), where SW is stroke work (the area in the pressure-volume loop), P_{ED} is end-diastolic pressure, P_{ES} is end-systolic pressure, V_{ED} is end-diastolic volume, and V_{ES} is end-systolic volume.

MVo_2 was calculated by the following equation: $MVo_2 = [Po_2$ (oxygenated perfusate) − Po_2 (coronary effluent)] × Bunsen solubility coefficient of O_2 × coronary flow. Po_2 was measured by the use of a fiber-optic oxygen sensor (FOXY-AL300; Ocean Optics), which was connected to a spectrophotometer (USB2000-FL-450; Ocean Optics) (2,8). Oxygen saturation of the coronary effluent was measured by placing the sensor in the opening of the pulmonary trunk.

Plasma analysis. After excision of the heart, a blood sample was taken from the chest cavity and quickly centrifuged; thereafter, the plasma was frozen at −70°C for later analysis. The plasma concentrations of glucose, fatty acids, and triacylglycerol were measured using commercial kits from Boehringer Mannheim (no. 1442449; Mannheim, Germany), Wako Chemicals (no. 994-75409; Neuss, Germany), and ABX Diagnostics (Montpellier, France), respectively.

Measurements of cardiac metabolism. In a separate set of experiments, fatty acid and glucose oxidation were measured as described in detail by Aasum et al. (9). Hearts were perfused in working mode for 40 min in the presence of 11 mmol/l glucose and either 0.3 or 1.4 mmol/l palmitate. Glucose oxidation was determined by measuring $^{14}CO_2$ released by the metabolism of [U-^{14}C]glucose. Palmitate oxidation was determined by measuring the amount of ^3H_2O released from [9,10-^{3}H]palmitate. Metabolic rates were calculated based on $^3H_2O/^{14}CO_2$ production and the specific activities of the radiolabeled substrates in the perfusate.

Isolation of mitochondria and measurement of respiration. Mitochondria were isolated, using the method of Sordahl et al. (10) with slight modifications. Mitochondrial protein concentrations were determined, using the method of Lowry et al. (11). Mitochondrial respiration (state 2, 3, and 4) was measured polarographically at 25°C, using an oxygraph (Hansatech Instruments, London). Mitochondrial respiration analyses were performed only when the respiratory control ratio was ≥3. Two sets of experiments were performed, using either pyruvate or L-palmitoyl-carnitine/malate as substrates.

Statistics. Differences in cardiac function in response to increasing workloads were determined by repeated-measures ANOVA followed by unpaired Student's t test for between-group analysis. Other data were assessed statistically by ANOVA followed by a paired (effect of elevated fatty acids within the same group) and/or unpaired (between groups) Student's t test. Bonferroni's method was applied in the case of multiple comparisons. $P < 0.05$ was considered statistically significant. All data are the means ± SE.

RESULTS

Characteristics of type 1 and type 2 diabetic mice. In accordance with previous results (9), *db/db* mice showed severe obesity and significantly elevated plasma concentrations of fatty acids and glucose, compared with nondiabetic controls (Table 1). Conversely, STZ-administered *db/+* mice displayed reduced body weight and no elevation in plasma fatty acids compared with nondiabetic controls. Nevertheless, the diabetic state was confirmed by significantly elevated plasma glucose concentrations (Table 1) as well as the appearance of ketone bodies in the urine (not shown). In addition, heart weights were significantly lower in STZ-administered mice compared with controls, as noted previously (4). Thus, despite similarities regarding the degree of hyperglycemia, the type 1 and type 2 diabetic mouse models used in this study displayed distinct metabolic signatures.

Cardiac metabolism and mitochondrial respiration are altered in hearts from type 1 and type 2 diabetic mice. Glucose and fatty acid oxidation rates from *db/+*, *db/db*, and STZ-administered *db/+* hearts are summarized in Fig. 2. Elevation of fatty acids in the perfusate (from 0.3 to 1.4 mmol/l) caused a marked shift in substrate utilization in control hearts. This can be seen by the eightfold increase in fatty acid oxidation combined with a marked reduction in glucose oxidation rates, reflecting metabolic control by the Randle cycle.

TABLE 1
Characteristics of control (*db/+*), type 2 (*db/db*), and type 1 (STZ-administered *db/+*) diabetic mice; body weights and dry heart weights; and plasma levels of glucose, free fatty acids, triglycerides, and insulin at time of death

Mice	Body weight (g)	Heart dry weight (mg)	Glucose (mmol/l)	Fatty acids (mmol/l)	Triglycerides (mmol/l)	Insulin (μg/l)
db/+	28.3 ± 0.7	30.5 ± 1.0	11.2 ± 0.4	0.51 ± 0.04	0.68 ± 0.07	1.20 ± 0.21
db/db	47.0 ± 0.8*	27.6 ± 0.4	32.2 ± 1.6*	1.03 ± 0.08*	0.89 ± 0.09	4.77 ± 0.83*
STZ	21.5 ± 0.6*	22.0 ± 0.4*	31.8 ± 1.8*	0.45 ± 0.06	0.57 ± 0.09	0.25 ± 0.04*

Data are means ± SE. n = 15–19, and n = 6–11 for the insulin values. *$P < 0.05$ vs. *db/+*.

Substrate utilization by *db/db* hearts clearly differed from control *db/+* hearts. At low fatty acid supply, glucose oxidation was markedly reduced, whereas fatty acid oxidation was fivefold elevated (Fig. 2). Perfusion of *db/db* hearts with an elevated perfusate fatty acid concentration produced a further increase in fatty acid oxidation and an additional decrease in glucose oxidation. The oxidation of fatty acids and glucose in hearts from STZ-administered mice was not different from control rates when perfused with low fatty acid supply (Fig. 2). However, there was a blunted response in the metabolic shift after elevation of fatty acids, as seen by only a 2.5-fold increase in fatty acid oxidation and a smaller reduction in glucose oxidation.

Respiration rates for mitochondria isolated from control, *db/db*, and STZ-administered hearts are shown in Table 2. State 3 respiration was elevated in *db/db* mitochondria incubated with palmitoyl-carnitine but not with pyruvate, consistent with the elevated rates of fatty acid oxidation observed with perfused *db/db* hearts (Fig. 2). In contrast, state 3 respiration was attenuated in type 1 (STZ-administered *db/+*) diabetic mouse mitochondria incubated with either palmitoyl-carnitine or pyruvate (Table 2).

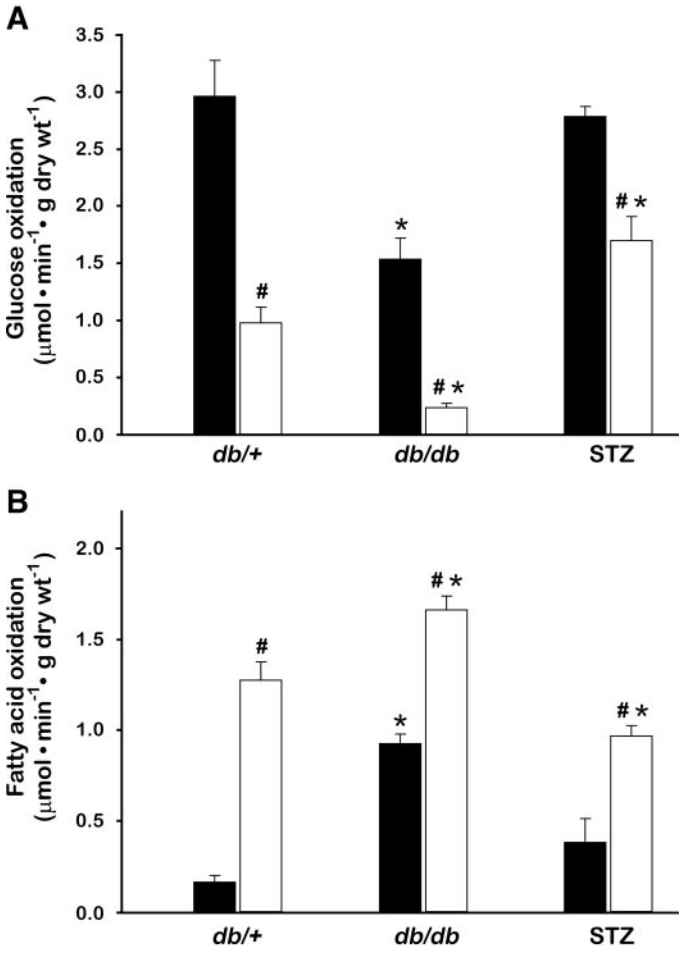

FIG. 2. Glucose and fatty acid oxidation rates were measured in hearts from control (*db/+*, n = 7), type 2 (*db/db*, n = 5), and type 1 (STZ-administered *db/+*, n = 9) diabetic mice, perfused with low and high fatty acid concentrations. *$P < 0.05$ vs. *db/+* hearts; #$P < 0.05$ vs. low fatty acids. ■, low fatty acid concentration; □, high fatty acid concentration.

Cardiac efficiency is reduced in type 1 and type 2 diabetic hearts. Exposure of perfused hearts to different loading conditions revealed a linear relationship between MVO_2 and cardiac work (PVA), as observed previously (2). Figure 3 shows pooled data points relating MVO_2 and PVA at increasing workloads in perfused working hearts from control, *db/db*, and STZ-administered mice. The data scatter includes 5–7 hearts from individual experiments listed in Table 3. Table 3 also gives the slope and y-intercept for the individual regression lines, as well as group means. The y-intercept (unloaded MVO_2) was significantly higher in both *db/db* and STZ-administered hearts compared with control hearts, indicating reduced cardiac efficiency in unloaded type 1 and type 2 diabetic hearts. At low fatty acid supply (0.3 mmol/l), hearts from *db/db* and STZ-administered mice consumed 86 and 57% more oxygen for noncontractile purposes, respectively, compared with control hearts (indicated by the y-intercept of the MVO_2-PVA regression lines in the upper panel of Fig. 3 as well as in Table 3).

At high fatty acid (1.4 mmol/l) supply, control hearts showed a relatively small (17%) but significant elevation in unloaded MVO_2 (Table 3); in contrast, increased fatty acid supply had no effect on the already elevated unloaded MVO_2 in *db/db* and STZ-administered hearts. However, unloaded MVO_2 was still significantly higher in diabetic hearts (both models) than in control hearts during high fatty acid supply. Strikingly, hearts from *db/db* mice showed a significant increase in the slope of the MVO_2-PVA regression line after the increase in perfusate fatty acids, which implies a reduction in contractile efficiency. The contractile efficiency of STZ hearts was unaffected by the changes in substrate supply.

The reduction in cardiac efficiency was most pronounced in *db/db* hearts (Table 3) and was consistent over a broad range of workloads (Fig. 3). In STZ-administered hearts, the more moderate decrease in cardiac efficiency diminished at increased workloads.

Ventricular function in perfused working hearts from type 1 and type 2 diabetic hearts. Stepwise changes in pre- and afterload settings revealed end-diastolic and end-systolic pressure-volume relationships (Fig. 4*A*). The ventricular function of *db/db* hearts differed substantially compared with the two other groups (Fig. 4*B*); at all steady states, the pressure-volume loop was shifted to the left in

TABLE 2
Respiration rates with different oxidative substrates for mitochondria isolated from control (*db/+*), type 2 (*db/db*), and type 1 (STZ-administered *db/+*) diabetic mice

	Pyruvate			Malate/carnitine-L-palmitoyl		
	db/+	*db/db*	STZ	*db/+*	*db/db*	STZ
State 2	16.9 ± 2.1	14.3 ± 1.2	15.2 ± 1.3	39.1 ± 2.7	37.8 ± 2.7	23.9 ± 4.5*
State 3	68.7 ± 11.0	53.1 ± 4.7	30.3 ± 4.0*	103.7 ± 23.5	157.9 ± 13.7*	56.3 ± 13.7
State 4	13.2 ± 3.6	9.2 ± 2.7	8.3 ± 4.9	22.6 ± 6.4	23.3 ± 5.5	13.3 ± 3.9

Data are means ± SE. Mitochondrial respiration was measured using either 7 mmol/l pyruvate or 25 μmol/l palmitoyl-carnitine/5 mmol/l malate as substrates (n = 5–8). The mitochondrial respiration data are expressed in nmol $O_2 \cdot min^{-1} \cdot mg\ protein^{-1}$. Basal (state 2) respiration was measured in the absence of added ADP; rates of state 3 respiration were recorded after the addition of 300 μmol/l ADP, whereas state 4 respiration was recorded after complete phosphorylation of added ADP. *$P < 0.05$ vs. *db/+*.

db/db hearts. Intrinsic heart rates in both diabetic models (*db/db* and STZ) were significantly reduced at all workloads (Fig. 5 and Table 4). Only *db/db* hearts, however, showed reduced cardiac output. In all groups cardiac function was unaffected by the elevation of fatty acids in the perfusate, except for a minor reduction in contractility in *db/db* hearts, shown by the small reduction in E_{max} (the slope of time-varying maximal ventricular elastance) and the preload recruitable stroke work index (Table 4). However, all hearts responded with increased MVo_2 after elevation of fatty acids, which was most evident in control hearts.

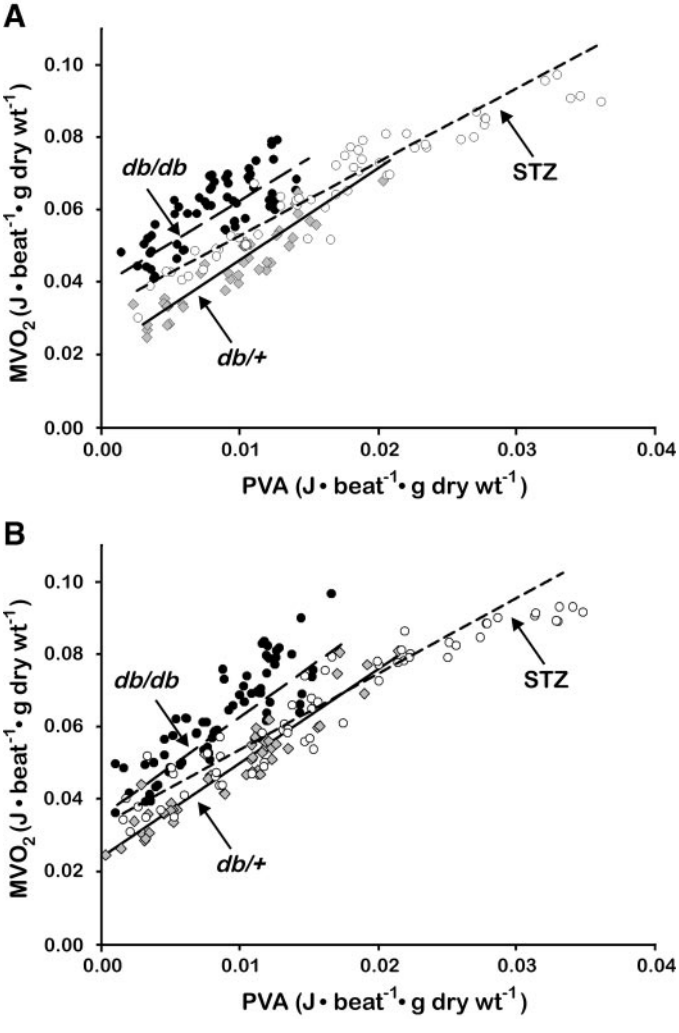

FIG. 3. Pooled scatter plot showing the relationship between MVo_2 and PVA at increasing workloads in hearts from control (*db/+*, n = 5), type 2 (*db/db*, n = 7), and type 1 (STZ-administered *db/+*, n = 7) diabetic mice. *A*: Data obtained at low fatty acid concentrations. *B*: Data obtained at high fatty acid concentrations. Each heart was subjected to different workloads by varying the preload (3–12.5 mmHg) and afterload (35–65 mmHg) settings. The regression line for each group is based on the average *y*-intercepts and slopes given in Table 3.

DISCUSSION

Measurements of MVo_2 (including any use of oxygen that might not be tightly coupled to oxidative phosphorylation) and PVA over a wide range of workloads are essential for a proper evaluation of cardiac efficiency. Reduced cardiac efficiency may be caused by an increase in unloaded MVo_2 (the *y*-intercept of the regression line), reflecting the oxygen cost of excitation-contraction coupling and/or basal metabolism. In addition, a reduction in contractile efficiency (increased slope of the regression line) can contribute to overall cardiac inefficiency. The current investigation tested the hypothesis that diabetic hearts exhibit reduced cardiac efficiency, using perfused working hearts from both type 1 (STZ-induced) and type 2 (*db/db*) diabetic mice.

Cardiac efficiency was reduced in type 2 diabetic hearts, as evidenced by the 86% increase in unloaded MVo_2 (Table 3). A likely explanation for this reduction in cardiac efficiency is the altered metabolism of *db/db* hearts (Fig. 2) because other investigations have shown that elevated rates of fatty acid uptake/oxidation produced an increase in unloaded MVo_2 in nondiabetic hearts from dog (12), pig (13), rat (14), and mouse (2). The extra oxygen cost of increased fatty acid oxidation relative to glucose oxidation will, however, make a minor contribution because there is only a theoretical 11% decrease in efficiency in hearts shifting from 100% glucose oxidation to 100% palmitate oxidation (15), an extreme condition that does not apply to the metabolic rates measured in perfused *db/db* hearts (Fig. 2). We therefore propose that intracellular futile metabolic cycles may also contribute to the increase in unloaded MVo_2 in *db/db* hearts. For example, with high intracellular fatty acid levels, a triacylglycerol–fatty acid cycle has been shown to increase oxygen consumption by up to 30% (16). Finally, peroxisome proliferator–activated receptor-α–dependent upregulation of mitochondrial uncoupling proteins induced by elevated plasma fatty acids (17) could dissipate the proton gradient across the inner mitochondrial membrane; uncoupling of electron flow from oxidative phosphorylation will reduce ATP synthesis and increase O_2 consumption (18). Examination of these mechanisms will be an important objective for future investigations.

An elevation in perfusate fatty acids to 1.4 mmol/l did not produce a further increase in unloaded MVo_2 in *db/db*

TABLE 3
Regression data for the PVA-MVO_2 relationships from individual experiments with hearts from control (*db/+*), type 2 (*db/db*), and type 1 (STZ-administered *db/+*) diabetic mice at low and high fatty acid perfusate

	Low fatty acids			High fatty acids		
	y-intercept · 10^{-2}	Slope	r^2	*y*-intercept · 10^{-2}	Slope	r^2
db/+						
1	2.5	1.8	0.83	2.5	2.0	0.98
2	2.0	2.4	0.95	2.4	2.6	0.93
3	1.8	3.2	0.97	2.1	3.1	0.98
4	1.4	2.8	0.91	1.9	2.8	0.95
5	2.9	2.1	0.86	3.1	2.5	0.93
Means ± SE	2.1 ± 0.3	2.5 ± 0.3	0.91 ± 0.03	2.4 ± 0.2*	2.6 ± 0.2	0.95 ± 0.01
db/db						
1	3.7	2.1	0.96	3.8	2.4	0.88
2	4.8	2.5	0.94	4.5	2.8	0.96
3	3.0	1.4	0.95	2.6	1.6	0.89
4	4.0	3.2	0.89	2.9	3.6	0.88
5	4.0	2.9	0.87	4.1	3.3	0.93
6	4.7	1.9	0.90	3.8	2.9	0.98
7	3.4	2.3	0.97	3.5	2.3	0.90
Mean ± SE	3.9 ± 0.3†	2.3 ± 0.3	0.92 ± 0.02	3.6 ± 0.3†	2.7 ± 0.3*	0.92 ± 0.02
STZ						
1	3.0	2.0	0.98	3.3	2.1	0.98
2	3.2	2.0	0.97	3.5	2.6	1.00
3	2.5	2.7	0.95	2.2	2.9	0.98
4	2.9	1.8	0.87	3.1	1.7	0.98
5	3.8	1.7	0.95	3.6	1.8	0.93
6	4.0	2.0	0.92	4.2	1.8	0.94
7	3.8	1.6	0.95	3.5	1.8	0.97
Mean ± SE	3.3 ± 0.2†	2.0 ± 0.1	0.94 ± 0.01	3.3 ± 0.3†	2.1 ± 0.2	0.97 ± 0.01

The *y*-intercept represents MVO_2 for unloaded hearts, expressed as Joules · $beat^{-1}$ · gram dry heart wt^{-1}. Slope is dimensionless, whereas r^2 is the square of the regression coefficient. Only experiments with a regression coefficient >0.9 ($r^2 \geq 0.81$) were included. *$P < 0.05$ vs. low fatty acids; †$P < 0.05$ vs. *db/+* hearts.

hearts (Table 3), even though fatty acid oxidation rates were enhanced (Fig. 2), suggesting that the contribution of fatty acid metabolism to cardiac inefficiency was already maximal in *db/db* hearts perfused at low fatty acid levels. On the other hand, *db/db* hearts perfused with 1.4 mmol/l fatty acids did exhibit a significant increase in the slope of the PVA-MVO_2 relationship (Table 3), indicating that a fatty acid–induced decrease in contractile efficiency could also contribute to the overall reduction in cardiac efficiency.

The decreased efficiency caused by elevated substrate fatty acids in the control hearts was the result of increased MVO_2, whereas ventricular work was unaffected (Tables 3 and 4). This suggests that the hearts were normoxic under all perfusion conditions because cardiac performance at high fatty acid supply is only impaired on insufficient oxygen delivery to the myocardium (12,14). Similarly, the decreased efficiency in *db/db* hearts was caused by elevated MVO_2. The findings in the current study are in contrast to a recent study by Mazumder et al. (19), where reduced cardiac efficiency in *ob/ob* hearts was caused by reduced ventricular work and elevated MVO_2. Nevertheless, results from the current investigation and Mazumder et al. (19) both support a common conclusion that cardiac efficiency is reduced in diabetic *db/db* and *ob/ob* hearts. In contrast, a study on type 2 diabetic ZDF rat hearts reported that cardiac efficiency was normal, despite elevated rates of fatty acid oxidation (20).

Alterations in metabolism related to hyperlipidemia (as described above) are probably not the only factor causing the pronounced oxygen waste in the unloaded *db/db* hearts. This is supported by the fact that STZ-administered hearts displayed a similar plasma fatty acid profile and cardiac oxidation pattern as controls, but they still had a 57% increase in unloaded MVO_2 (Table 3). The increased unloaded MVO_2 in these diabetic hearts could therefore not be explained in terms of elevated fatty acid oxidation.

Unloaded MVO_2 consists of two components: basal metabolism and the oxygen cost of excitation-contraction coupling. Several studies have shown that high extracellular Ca^{2+} concentration or β-adrenergic stimuli increased the oxygen cost for excitation-contraction coupling and consequently elevated unloaded MVO_2 (21); conversely, low Ca^{2+} concentration or a calcium antagonist decreased unloaded MVO_2 (22). It is reasonable to suggest, therefore, that abnormal Ca^{2+} homeostasis as shown in diabetic hearts (23) could contribute to the increased unloaded MVO_2 in hearts from both of the diabetic models.

The decreased cardiac efficiency in hearts from STZ-administered *db/+* mice, manifested by an increase in unloaded MVO_2, contrasts with data obtained with diabetic hearts from STZ-administered sheep (24), in which decreased cardiac efficiency was the result of impaired contractile efficiency with no change in unloaded MVO_2. In fact, the slope of the PVA-MVO_2 relationship for STZ-administered mouse hearts was the lowest (Table 3). Diabetic sheep had elevated plasma fatty acids and increased cardiac fatty acid uptake (24), a metabolic profile that is more similar to *db/db* mice.

The metabolic phenotype of diabetic hearts will reflect, in part, an adaptation to chronic changes in substrate supply in vivo (25). Type 2 diabetic *db/db* mice have elevated plasma lipids (Table 1) (3). Thus, oversupply of

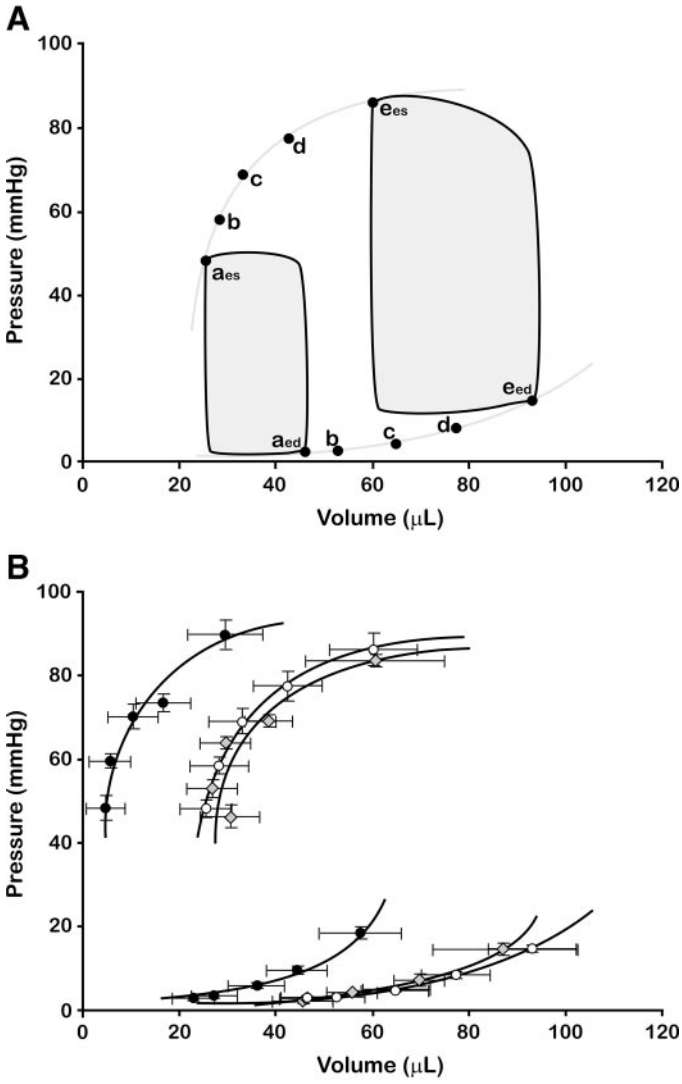

FIG. 4. *A*: Steady-state pressure-volume loops in a representative heart obtained at increasing pre- and afterload settings (a: 3 and 35 mmHg; b: 4 and 45 mmHg; c: 6 and 50 mmHg; d: 8 and 50 mmHg; e: 12.5 and 65 mmHg). For simplicity, only loops at the highest and lowest workloads are illustrated. $a_{ed/es}$ and $e_{ed/es}$ denote the corresponding end-diastolic and -systolic pressure-volume relationships, respectively. End-diastolic and -systolic pressure-volume relationships at intermediary workloads (b–d) are also indicated. *B*: End-diastolic and -systolic pressure-volume relationships obtained in hearts from control (*db/+*, $n = 7$), type 2 (*db/db*, $n = 8$), and type 1 (STZ-administered *db/+*, $n = 7$) diabetic mice over the same range of pre- and afterload settings as in *A*. Gray ◇, control mice; ●, type 2 diabetic mice; ○, type 1 diabetic mice.

fatty acids to *db/db* hearts will unquestionably be a factor in subsequent metabolic alterations, namely decreased glucose utilization and increased fatty acid oxidation (Fig. 2). It should be noted, however, that the absence of a functional leptin receptor in the *db/db* mouse could impair insulin sensitivity independently of hyperglycemia and hyperlipidemia, and extrapolation to type 2 diabetes in obese humans demands caution. Moreover, STZ treatment of *db/+* mice produced an equivalent degree of hyperglycemia (confirming their insulin-deficient diabetic status), although plasma lipids were not elevated (Table 1). This somewhat surprising finding is most likely related to the duration and/or severity of the diabetic state; the animals showed a significant reduction in body weight, and visible fat was virtually absent at the time of death, which excludes mobilization of fatty acids from endogenous sources. Thus, the absence of any change in lipid substrate supply in vivo may explain the absence of any alteration in glucose and fatty acid oxidation (Fig. 2). Interestingly, the increase in fatty acid oxidation and suppression of glucose oxidation caused by the elevation in perfusate fatty acids in STZ-induced diabetic hearts was blunted compared with control or *db/db* hearts (Fig. 2), indicating that short-term (2 weeks) insulin deficiency had altered the metabolic phenotype of the mouse hearts. Finally, it must be acknowledged that results shown in Fig. 2 for hearts from STZ-administered *db/+* mice are not consistent with a previous study by Neitzel et al. (4) that reported elevated palmitate oxidation by perfused hearts from STZ-administered *db/+* mice. However, these authors did not measure glucose oxidation or plasma lipids; therefore, there may be differences in the type 1 diabetic model.

The observation that state 3 respiration by *db/db* mitochondria was elevated in the presence of palmitoyl-carnitine (Table 2) is consistent with enhanced rates of fatty acid oxidation measured with perfused *db/db* hearts. Respiration in mitochondria from STZ-administered hearts was generally impaired, with a significant reduced state 3 when pyruvate was used as substrate, indicating mitochondrial dysfunction (Table 2). STZ-administered *db/+* mice also had decreased body weight and heart weight (Table 1), and this observation supports previous data by Lashin and Romani (26) that mitochondrial dysfunction in STZ-administered rat hearts required not only hyperglycemia but other signs of diabetes, such as weight loss. It cannot be excluded, however, that isolation of mitochondria from the more fragile STZ-administered hearts resulted in a lower fraction of intact mitochondria, which in turn could explain the impaired respiration in these preparations.

Previous studies have shown that *db/db* hearts exhibit a progressive age-dependent decline in contractile performance (3). The ability to obtain instantaneous pressure-volume loops in perfused mouse hearts has provided new mechanistic insights into alterations in ventricular function. Thus, the current study revealed that the end-diastolic, as well as the end-systolic, pressure-volume relationships for *db/db* hearts were markedly shifted to the left (Fig. 4) relative to control hearts. The interpretation of this finding is not obvious, but ventricular remodeling with concentric hypertrophy and/or reduced compliance because of myocardial fibrosis seems plausible. In accordance with the review by Cosson and Kevorkian (27), hearts from *db/db* mice also showed signs of diastolic dysfunction; the increased Tau value (Table 4) is indicative of an abnormal calcium reuptake into the sarcoplasmic reticulum (23), resulting in impaired relaxation in early diastole. In addition, the slope of the end-diastolic pressure-volume relationship and end-diastolic pressure was clearly increased for *db/db* hearts, indicating ventricular chamber stiffness and dysfunction also in late diastole (Figs. 4 and 5). The underlying mechanisms of these diastolic abnormalities and their potential contribution to the onset of heart failure, as reviewed by Kass et al. (28), require further investigations.

Elevation of perfusate fatty acids did not significantly affect cardiac performance in either control or diabetic hearts, except for a small decrease in contractility (reduced preload recruitable stroke work index and E_{max}) in *db/db* hearts (Table 4) associated with the reduction in contractile efficiency (increased slope of the PVA-MVo_2

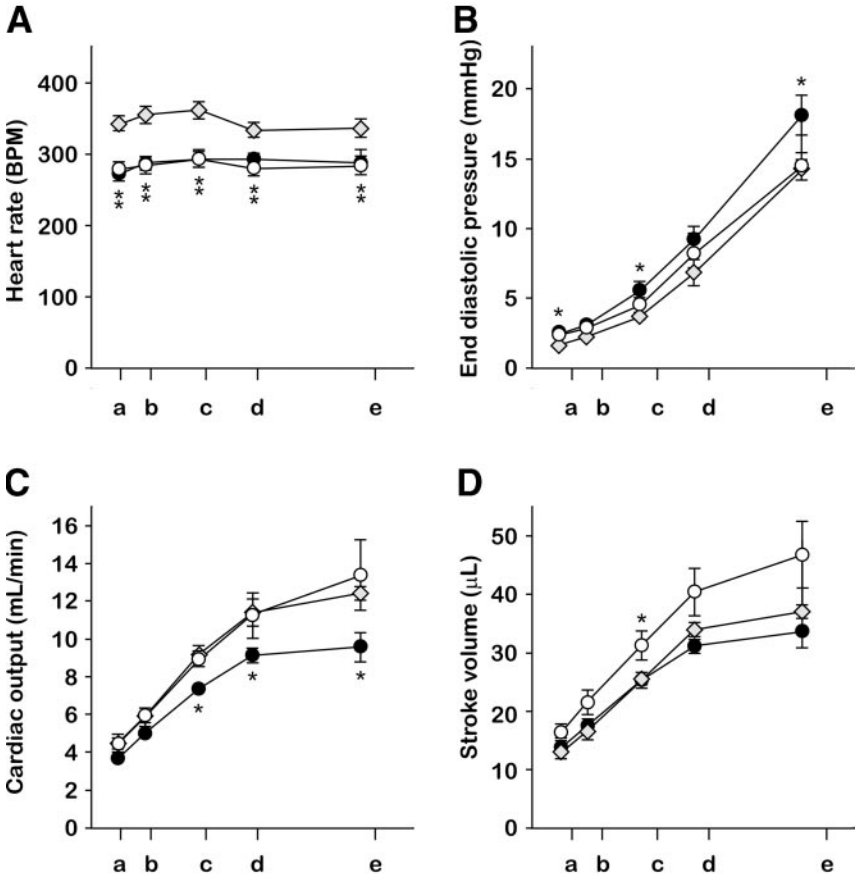

FIG. 5. Heart rate (*A*), end-diastolic pressure (*B*), cardiac output (*C*), and stroke volume (*D*) at increasing pre- and afterload settings in the same hearts as those referred to in Fig. 4. *$P < 0.05$ vs. *db/+* hearts.

relationship) (Table 3). As mentioned above, these results are clearly in contrast to the marked decline in cardiac function in hearts from *ob/ob* mice after elevation in perfusate fatty acids (19). The slightly reduced preload recruitable stroke work index and E_{max} values of the *db/db* hearts after elevation of fatty acids are probably a consequence of altered calcium homeostasis (23). However, further investigations are required to reveal the impact of fatty acids on contractility in the diabetic heart.

Intrinsic heart rates in both diabetic models (*db/db* and STZ) were significantly lower compared with control heart rates (Fig. 5 and Table 4). In STZ hearts, prolonged diastolic filling time resulted in elevation of stroke volume that compensated for reduced heart rates, so that cardiac output was similar to control. The *db/db* hearts, however, had no increase in stroke volume, despite the reduced heart rates and thus reduced cardiac output compared with controls, suggesting reduced compliance in the *db/db* left ventricle. This reduced compliance corresponded with an elevation in end-diastolic pressure (Fig. 5) in *db/db*

TABLE 4
Effects of elevated fatty acid supply on ventricular function in perfused working hearts from control (*db/+*), type 2 (*db/db*), and type 1 (STZ-administered *db/+*) diabetic mice

	db/+ ($n = 6$)		*db/db* ($n = 8$)		STZ ($n = 7$)	
	Low fatty acids	High fatty acids	Low fatty acids	High fatty acids	Low fatty acids	High fatty acids
Heart rate (bpm)	334 ± 11	320 ± 18	295 ± 12	281 ± 12	279 ± 13	281 ± 12
End-systolic pressure (mmHg)	69 ± 2	70 ± 2	74 ± 3	76 ± 2	77 ± 4	77 ± 3
End-diastolic pressure (mmHg)	7 ± 1	8 ± 1	9 ± 1	10 ± 1	8 ± 1	9 ± 1
dP/dt_{max} (mmHg/s)	4,935 ± 199	5,005 ± 248	5,483 ± 343	5,499 ± 207	5,419 ± 292	5,315 ± 385
dP/dt_{min} (mmHg/s)	−4,352 ± 203	−4,152 ± 257	−4,682 ± 264	−4,451 ± 254	−4,943 ± 187	−4,857 ± 296
Tau (ms)	15 ± 1	15 ± 1	18 ± 3	20 ± 3	13 ± 1	14 ± 1
Cardiac output (ml/min)	11.4 ± 0.7	10.8 ± 0.7	9.4 ± 0.3	9.4 ± 0.3	11.3 ± 1.2	11.5 ± 1.2
Coronary flow rate (ml/min)	2.5 ± 0.4	2.6 ± 0.5	2.1 ± 0.1	2.2 ± 0.1	2.3 ± 0.2	2.4 ± 0.2
E_{max}	3.4 ± 0.3	3.7 ± 0.6	6.6 ± 0.9	5.6 ± 0.9*	3.6 ± 0.5	3.4 ± 0.4
PRSWi	51.5 ± 3.7	45.6 ± 6.2	57.3 ± 3.2	48.3 ± 5.4*	50.3 ± 2.5	46.9 ± 3.6
EDPVR · 10^{-2}	6.5 ± 0.6	6.7 ± 0.9	9.2 ± 1.1	8.6 ± 1.1	5.3 ± 0.4	5.7 ± 0.6

Parameters of cardiac function were measured with low and high fatty acid concentrations (before and after the buffer replacement) in working hearts at 8 mmHg preload and 50 mmHg afterload. The relaxation constant Tau (glanz) is the regression of dP/dt versus pressure. The time-varying maximal ventricular elastance (E_{max}), preload recruitable stroke work index (PRSWi), and exponential fit of the relationship between pressure and volume at end diastole (EDPVR) were assessed from a family of pressure-volume loops created by a temporary preload occlusion. *$P < 0.05$ vs. low fatty acids.

hearts. Thus, *db/db* hearts have impaired diastolic properties that are revealed at high workloads. Comparison of ventricular function at different heart rates is problematic because several functional parameters are heart rate–dependent. However, pacing electrodes markedly influence the conductance signal of the high-fidelity pressure-volume catheter.

In summary, this is the first study showing decreased cardiac efficiency in hearts from diabetic mice (both type 1 and type 2) assessed by the MVO_2-PVA relationship. This inefficiency was revealed as a pronounced oxygen waste in the unloaded heart, which may compromise ventricular function when oxygen demand is high (elevated workloads) or when oxygen delivery is limited (ischemic insult).

ACKNOWLEDGMENTS

This work was supported by operating grants from the Norwegian Heart Foundation (6426) and the Norwegian Research Council (148192/310 and 152269/730).

The assistance by the technical staff at the Department of Medical Physiology is gratefully acknowledged.

REFERENCES

1. Suga H: Total mechanical energy of a ventricle model and cardiac oxygen consumption. *Am J Physiol* 236:H498–H505, 1979
2. How OJ, Aasum E, Kunnathu S, Severson DL, Myhre ES, Larsen TS: Influence of substrate supply on cardiac efficiency, as measured by pressure-volume analysis in ex vivo mouse hearts. *Am J Physiol Heart Circ Physiol* 288:H2979–H2985, 2005
3. Aasum E, Hafstad AD, Severson DL, Larsen TS: Age-dependent changes in metabolism, contractile function, and ischemic sensitivity in hearts from db/db mice. *Diabetes* 52:434–441, 2003
4. Neitzel AS, Carley AN, Severson DL: Chylomicron and palmitate metabolism by perfused hearts from diabetic mice. *Am J Physiol Endocrinol Metab* 284:E357–E365, 2003
5. Kennedy JM, Zochodne DW: The regenerative deficit of peripheral nerves in experimental diabetes: its extent, timing and possible mechanisms. *Brain* 123:2118–2129, 2000
6. Baan J, van der Velde ET, de Bruin HG, Smeenk GJ, Koops J, van Dijk AD, Temmerman D, Senden J, Buis B: Continuous measurement of left ventricular volume in animals and humans by conductance catheter. *Circulation* 70:812–823, 1984
7. Korvald C, Elvenes OP, Ytrebo LM, Sorlie DG, Myrmel T: Oxygen-wasting effect of inotropy in the "virtual work model." *Am J Physiol* 276:H1339–H1345, 1999
8. Zhao Y, Richman A, Storey C, Radford NB, Pantano P: In situ fiber-optic oxygen consumption measurements from a working mouse heart. *Anal Chem* 71:3887–3893, 1999
9. Aasum E, Belke DD, Severson DL, Riemersma RA, Cooper M, Andreassen M, Larsen TS: Cardiac function and metabolism in type 2 diabetic mice after treatment with BM 17.0744, a novel PPAR-alpha activator. *Am J Physiol Heart Circ Physiol* 283:H949–H957, 2002
10. Sordahl LA, Besch HR Jr, Allen JC, Crow C, Lindenmayer GE, Schwartz A: Enzymatic aspects of the cardiac muscle cell: mitochondria, sarcoplasmic reticulum and nonovalent cation active transport system. *Methods Achiev Exp Pathol* 5:287–346, 1971
11. Lowry OH, Roseburgh NJ, Farr Al, Randall RJ: Protein measurement with the Folin phenol reagent. *J Biol Chem* 193:265–275, 1951
12. Mjos OD: Effect of free fatty acids on myocardial function and oxygen consumption in intact dogs. *J Clin Invest* 50:1386–1389, 1971
13. Korvald C, Elvenes OP, Myrmel T: Myocardial substrate metabolism influences left ventricular energetics in vivo. *Am J Physiol Heart Circ Physiol* 278:H1345–H1351, 2000
14. Burkhoff D, Weiss RG, Schulman SP, Kalil-Filho R, Wannenburg T, Gerstenblith G: Influence of metabolic substrate on rat heart function and metabolism at different coronary flows. *Am J Physiol* 261:H741–H750, 1991
15. Opie LH: *Heart Physiology*: *From Cell to Circulation*. Philadelphia, PA, Lippincott Williams and Wilkins, 2004, p. 279–431
16. Myrmel T, Forsdahl K, Larsen TS: Triacylglycerol metabolism in hypoxic, glucose-deprived rat cardiomyocytes. *J Mol Cell Cardiol* 24:855–868, 1992
17. Murray AJ, Anderson RE, Watson GC, Radda GK, Clarke K: Uncoupling proteins in human heart. *Lancet* 364:1786–1788, 2004
18. Boehm EA, Jones BE, Radda GK, Veech RL, Clarke K: Increased uncoupling proteins and decreased efficiency in palmitate-perfused hyperthyroid rat heart. *Am J Physiol Heart Circ Physiol* 280:H977–H983, 2001
19. Mazumder PK, O'Neill BT, Roberts MW, Buchanan J, Yun UJ, Cooksey RC, Boudina S, Abel ED: Impaired cardiac efficiency and increased fatty acid oxidation in insulin-resistant *ob/ob* mouse hearts. *Diabetes* 53:2366–2374, 2004
20. Wang P, Lloyd SG, Zeng H, Bonen A, Chatham JC: Impact of altered substrate utilization on cardiac function in isolated hearts from Zucker diabetic fatty rats. *Am J Physiol Heart Circ Physiol* 288:H2102–H2110, 2005
21. Suga H, Hisano R, Goto Y, Yamada O, Igarashi Y: Effect of positive inotropic agents on the relation between oxygen consumption and systolic pressure volume area in canine left ventricle. *Circ Res* 53:306–318, 1983
22. Burkhoff D, Gerstenblith G: Impact of isradipine on contractile performance, metabolism, and coronary resistance studied in isolated rat hearts. *J Cardiovasc Pharmacol* 24:344–349, 1994
23. Belke DD, Swanson EA, Dillmann WH: Decreased sarcoplasmic reticulum activity and contractility in diabetic *db/db* mouse heart. *Diabetes* 53:3201–3208, 2004
24. Ramanathan T, Shirota K, Morita S, Nishimura T, Huang Y, Zheng X, Hunyor S: Left ventricular oxygen utilization efficiency is impaired in chronic streptozotocin-diabetic sheep. *Cardiovasc Res* 55:749–756, 2002
25. Young ME, McNulty P, Taegtmeyer H: Adaptation and maladaptation of the heart in diabetes. Part II. Potential mechanisms. *Circulation* 105:1861–1870, 2002
26. Lashin O, Romani A: Hyperglycemia does not alter state 3 respiration in cardiac mitochondria from type-I diabetic rats. *Mol Cell Biochem* 267:31–37, 2004
27. Cosson S, Kevorkian JP: Left ventricular diastolic dysfunction: an early sign of diabetic cardiomyopathy? *Diabetes Metab* 29:455–466, 2003
28. Kass DA, Bronzwaer JG, Paulus WJ: What mechanisms underlie diastolic dysfunction in heart failure? *Circ Res* 94:1533–1542, 2004